Numerical Modeling of Multiple Bubbles Condensation in Subcooled Flow Boiling

Zhenyu Liu
School of Mechanical Engineering,
Shanghai Jiao Tong University,
Shanghai 200240, China

Bengt Sunden[1]
Department of Energy Sciences,
Lund University,
Lund SE-221 00, Sweden
e-mail: bengt.sunden@energy.lth.se

Huiying Wu
School of Mechanical Engineering,
Shanghai Jiao Tong University,
Shanghai 200240, China

The understanding of multiple bubbles condensation is of significant importance in developing continuum models for the large-scale subcooled flow boiling. The computational fluid dynamics (CFD) modeling for multiple bubbles condensation is developed with the volume of fluid (VOF) method in this work. An explicit transient simulation is performed to solve the governing equations including the source terms for heat and mass transfer due to condensation. The geometric reconstruction scheme, which is a piecewise linear interface calculation (PLIC) method, is employed to keep the interface sharp. The surface tension is modeled by the continuum surface force (CSF) approach, which is taken into account in the numerical model. Numerical simulations predict the dynamical behavior of the actual condensing bubbles. The results show that the condensation rate of a single bubble is influenced by the velocity of the fluid flow and the temperature difference between the bubble and fluid. For multiple bubbles, the effect of bubble–bubble interaction on their condensation process is analyzed based on the numerical predictions. The condensation rate of lower bubbles increases due to the random perturbation induced by other bubbles. The influence of other bubbles on the condensation rate can be neglected if the distances between the bubbles are large enough. [DOI: 10.1115/1.4029953]

Introduction

Subcooled boiling occurs as the liquid temperature is below the saturation temperature. In many industrial applications, such as electronics cooling and nuclear engineering, the subcooled boiling flow has been studied as an important issue for the optimum design and safety analysis [1]. The subcooled boiling flow is a complex phenomenon due to the bubble–liquid and bubble–bubble interactions, which includes break-up, merging, and condensation of bubbles. Steam bubble condensation is one of the fundamental and challenging issues in the field of two-phase flow, and it has attracted more and more attention during recent years.

Several experimental studies have been conducted on the characteristics analysis of bubble condensation. In Kim and Park's research [2], the experiments were carried out to correlate the interfacial heat transfer coefficient at low pressure in the subcooled boiling flow. The condensation Nusselt number, which is a function of bubble Reynolds number, local liquid Prandtl number, and local Jacob number, was obtained from the experimental results. Lucas and Prasser [3] investigated the structure of a steam–water flow in a vertical pipe using novel wire-mesh sensors for high-pressure and high-temperature operation. It was found that bubble break-up has a strong influence on the condensation process because of the change of the interfacial area. The effect of bubble sizes was clearly shown in experimental investigations performed at the TOPFLOW facility by Lucas et al. [4]. Data on averaged void fraction, radial gas volume fraction profiles, gas velocity profiles, bubble size distributions, and the dependence on the length/diameter ratio were presented in their paper. Inaba et al. [5] experimentally measured the interfacial heat transfer coefficient of condensation bubble with consideration of bubble number distribution in subcooled flow boiling. In their report, the bubble number distributions, void fraction, bubble collapse rate, and phase change rate were investigated through the measurement of average interfacial heat transfer coefficient with image analysis, which was under the condition of forced convectional subcooled flow boiling.

However, it is impossible to obtain all details of the bubbles behavior because of the complexity of the vapor–liquid interface. The shape and the vapor–liquid interface, which govern the bubble behavior, are too complicated and difficult to be analyzed. It becomes more challenging to experimentally analyze the behavior of condensing bubble as it exists in a subcooled boiling flow. Therefore, it is necessary to perform numerical simulation as a complement to the experimental study on bubble behavior. Single steam bubble condensation behavior in subcooled water has been simulated using moving particle semi-implicit method by Tian et al. [6]. Jeon et al. [7] performed direct numerical simulation for the bubble condensation in the subcooled boiling flow. The amount of condensation was determined using the interfacial heat transfer coefficient obtained from the bubble velocity, liquid temperature, and bubble diameter every time step. Eames [8] categorized the possible mechanisms that lead to the generation of a vortex by bubbles. Lucas et al. [9] focused on the derivation of equations for the extension of the inhomogeneous MUSIG model and presented some first results for the verification and validation. Ganguli et al. [10] carried out experimental and numerical investigation on the bubble dynamics of a single condensing vapor bubble from vertically heated wall in subcooled pool boiling flow. The heat source was modeled using a simple heat balance and the rising behavior of condensing bubbles (change in size during rise and path tracking) was studied. Numerical simulation of multiple bubbles condensation can contribute to a better understanding of the complex phenomena for subcooled flow boiling, but only few related works, Refs. [7–13], have been found in the open literature.

The multiple bubbles condensation exists in the heat transfer equipment and has impact on the equipment performance. Bubble condensation is a key parameter to describe the heat transfer phenomenon in the subcooled flow boiling. A literature survey found only very few reports, Refs. [7–13], being relevant for the present work on numerical analysis of condensation of multiple bubbles. In this paper, the focus is put on how to simulate the bubble condensation with a CFD approach. The bubbles experience condensation as they rise in the low temperature liquid flow. For the behavior of condensing vapor bubbles, the VOF model was

[1]Corresponding author.

Contributed by the Heat Transfer Division of ASME for publication in the Journal of Thermal Science and Engineering Applications. Manuscript received October 28, 2014; final manuscript received January 23, 2015; published online April 8, 2015. Assoc. Editor: Mohamed S. El-Genk.

adopted in the simulation. In order to simulate the heat and mass transfer through the bubble interface, the condensation source terms were developed by an in-house code. The effect of the bubbles interaction on the condensation process was analyzed based on the numerical predictions in this study.

Mathematical Modeling and Assumptions

Governing Equations and VOF Model. The VOF method, which is a kind of Eulerian method, has been widely used in predicting two-phase fluid flow. The VOF formulation relies on the fact that two or more fluids are immiscible. For each phase considered in the model, a variable is introduced as the volume fraction of the phase in the computational cell. In each of the control volumes, the volume fractions of all phases sum to unity. The simulation work by Gopala and van Wachem [14] examined the applicability of the VOF model to the analysis of a single rising bubble in liquid, which confirmed that the VOF model can achieve good predictions of the bubble shape and terminal velocity. In the study of Rabha and Buwa [15], the VOF method was adopted to simulate the rising behavior of single and multiple bubbles in liquids of different properties imposed with linear shear.

As the VOF multiphase flow model is applied for two-phase flow, both phases are treated as noninterpenetrating and the flow behavior is described by Navier–Stokes equations. For a system with two incompressible fluids, the equations for conservation of mass, momentum, and energy are

$$\frac{\partial \rho}{\partial t} + \mathrm{div}(\rho \mathbf{V}) = 0 \tag{1}$$

$$\frac{\partial(\rho u)}{\partial t} + \mathrm{div}(\rho u \mathbf{V}) = -\frac{\partial p}{\partial x} + \mathrm{div}(\mu\, \mathrm{grad}\, u) + f_x \tag{2}$$

$$\frac{\partial(\rho v)}{\partial t} + \mathrm{div}(\rho v \mathbf{V}) = -\frac{\partial p}{\partial y} + \mathrm{div}(\mu\, \mathrm{grad}\, v) + f_y \tag{3}$$

$$\frac{\partial(\rho w)}{\partial t} + \mathrm{div}(\rho w \mathbf{V}) = -\frac{\partial p}{\partial z} + \mathrm{div}(\mu\, \mathrm{grad}\, w) - \rho g + f_z \tag{4}$$

$$\frac{\partial(\rho c_p T)}{\partial t} + \mathrm{div}(\rho c_p T \mathbf{V}) = \mathrm{div}(k\, \mathrm{grad}\, T) + q_T \tag{5}$$

In this study, the liquid and vapor are set as the primary and secondary phase, respectively. The momentum equations are solved throughout the domain, and the resulting velocity field is shared among the phases. Tracking of the interface between the phases is accomplished by the solution of a continuity equation for the volume fraction of the secondary phase, the VOF equation is written as

$$\frac{\partial F_v}{\partial t} + \mathrm{div}(F_v \mathbf{V}) = -\frac{\dot{m}_c}{\rho_v} \tag{6}$$

where $\dot{m}_c$ represents the mass production rate of condensation, and F_v is the volume fraction factor of vapor. If $F_v = 1$, the region is pure vapor, and if $F_v = 0$ then the region is pure liquid. F_v can also assume values between 0 and 1, which is defined as the mixture region of the phases and $F_v + F_l = 1$. All physical properties are volume-fraction-averaged ones.

Mass and Energy Transfer During the Condensation Process. In the subcooled boiling flow, bubble condensation is the key characteristic to describe heat and mass transfer phenomena. It significantly affects the shape and the area of the varying interface thus the behavior of the condensing bubble becomes different from that of the adiabatic one. Therefore, in order to understand bubble behavior in subcooled boiling flow, the heat and mass transfer through the interface should be considered before the numerical simulation.

For phase change problems, the critical issue is how to calculate the condensation rate $\dot{m}_c$, and the phase change related heat rate q_T. $\dot{m}_c$ represents the mass production rate due to condensation (positive value). q_T is the heat per unit volume due to the phase change process, whose value is always positive for condensation. The relationship between $\dot{m}_c$ and q_T is

$$\dot{m}_c = q_T / L \tag{7}$$

Here, L is latent heat. The expression (8) for the heat and mass transfer through the phase interface is used to model the bubble condensation

$$\dot{Q} = h_i A_b (T_{sat} - T_l) = \dot{M}_c L \tag{8}$$

where h_i is the interfacial heat transfer coefficient or condensation heat transfer coefficient, T_{sat} and T_l are the vapor and liquid temperatures, respectively, A_b is the interfacial or surface area of the bubble, and $\dot{M}_c$ is the total mass transfer rate. The condensation heat transfer coefficients h_i are assumed to have the following form:

$$\mathrm{Nu}_c = \frac{h_i D_s}{k_l} = f(\mathrm{Re}_b, \mathrm{Pr}_l, \mathrm{Ja}, \mathrm{Fo}_{bo}) \tag{9}$$

There are several correlations available based on experimental data [7,12,16],

$$\mathrm{Nu}_c = 0.2575 \mathrm{Re}_b^{0.7} \mathrm{Ja}_l^{-0.2043} \mathrm{Pr}_l^{-0.4564} \tag{10}$$

$$\mathrm{Nu}_c = 0.6 \mathrm{Re}_b^{0.5} \mathrm{Pr}_l^{-0.3333} (1 - \mathrm{Ja}^{0.1} \mathrm{Fo}_{bo}) \tag{11}$$

$$\mathrm{Nu}_c = 0.6 \mathrm{Re}_b^{0.5} \mathrm{Pr}_l^{-0.3333} (1 - 1.2 \mathrm{Ja}^{1/9} \mathrm{Fo}_{bo}^{2/3}) \tag{12}$$

The total mass transfer rate $\dot{M}_c$ is defined as the sum of mass transfer rate in each interface-cell, the average mass transfer rate $\dot{m}_c$ equals the overall mass transfer rate divided by the total vapor volume in the bubble interface region. The different ways to describe the condensation source terms were summarized by Liu et al. [17], and all these methods should be available to simulate the condensation process. Considering the issue of convergence, the source term based on the kinetic gas theory is adopted in this study.

The mass transfer due to phase change is introduced in the VOF equation via a source term. In order to correctly add this source term, the mass flux should be expressed in kg/m^3. The condensation source term can be expressed as in Ref. [17].

$$\dot{m}_c = \alpha_i \alpha_c \sqrt{\frac{M}{2\pi R T_{sat}}} \frac{L}{\left(\frac{1}{\rho_v} - \frac{1}{\rho_l}\right)} \frac{T - T_{sat}}{T_{sat}} \tag{13}$$

The volumetric interfacial surface area $\alpha_i = 6F_v/D_{sm}$, which is related to the mean Sauter diameter D_{sm} and the volume fraction of vapor F_v. Under the assumption that the accommodation coefficient α_c has a value of 1.0, which should be less than unity when the working fluids or the interface is contaminated, Eq. (13) for the volumetric interfacial surface area, the expression for the mass flux over the liquid–vapor interface, can be written as

$$\dot{m}_c = \beta_c F_v \rho_v \frac{T_{sat} - T}{T_{sat}} \tag{14}$$

In this study, the interfacial temperature is assumed as the saturation temperature ($T_{sat} = 373$ K). Excessively a large β_c causes a numerical convergence problem, while a too small value leads to a significant deviation between the interfacial temperature and the saturation temperature. For this purpose, the coefficient β_c is hereby specified at 5000 s^{-1} in order to numerically maintain the interface temperature close to saturation temperature.

The heat transfer is simply determined from the mass flow rate of condensation. As long as the mass transfer rate is obtained, the source term for the energy equation can be directly determined by Eq. (7).

Interfacial Surface Tension Evaluation. The CSF model was adopted in this study [18]. Its effect of the radial component of the force across the entire surface is to make the surface to contract and increase the pressure within the vapor phase. In the regions where two fluids are separated, the surface tension acts to minimize the free energy by decreasing the area of the interface, which is a force at the surface balancing the radially inward intermolecular attractive force with the radially outward pressure gradient force across the surface. In the CSF model, the addition of the surface tension to the VOF calculation results in a source term in the momentum equation. The pressure difference across the surface depends on the surface tension coefficient and the surface curvature as measured by two radii in orthogonal directions, r_1 and r_2

$$\Delta p = p_v - p_l = \sigma\kappa \tag{15}$$

in the above equation, Δp is the pressure drop across the interface, σ is the liquid surface tension coefficient, and $\kappa = (1/r_1 + 1/r_2)$ is the mean curvature. In the CSF model, the normal vector on an interface is defined as the gradient of F

$$\mathbf{n} = \nabla F \tag{16}$$

The curvature κ is represented by the divergence of the unit normal as

$$\kappa = \nabla \cdot \frac{\nabla F}{|\nabla F|} \tag{17}$$

The force at the surface can be expressed as a volume force using the divergence theorem, which is the source term added to the momentum equation

$$F_{\text{vol}} = \sum_{\text{pairsij},i<j} \sigma_{ij} \frac{F_i\rho_i\kappa_j\nabla F_j + F_j\rho_j\kappa_i\nabla F_i}{0.5(\rho_i + \rho_j)} \tag{18}$$

for the cases where only two phases (vapor and liquid) are present in an interfacial cell, $\kappa_v = -\kappa_l$ and $\nabla F_v = -\nabla F_l$, Eq. (18) can be simplified as

$$F_{\text{vol}} = 2\sigma_{lv} \frac{\rho\kappa_v\nabla F_v}{(\rho_v + \rho_l)} \tag{19}$$

where $\rho = F_v\rho_v + F_l\rho_l$. The initial pressure in the bubble is determined by Young–Laplace equation as follows:

$$p_v = p_l + \frac{2\sigma}{r} \tag{20}$$

Computational Domain and Strategy. In the present work, a rectangular domain with a square cross section was adopted, as shown in Fig. 1. The dimensions of the channel were 15 mm $\times$ 15 mm $\times$ 60 mm, and the flow direction was upward. The lateral wall was a rigid insulated boundary, the bottom was velocity inlet boundary, and the top was pressure outlet boundary. The initial and boundary conditions, such as the liquid velocity and bubble region, were set using user defined function (UDF) in ANSYS-FLUENT. The inlet and local liquid velocity distribution was specified by the profile in parabolic shape.

A numerical test was performed at the beginning, the double-precision was adopted in all conditions in the present work. The vapor and liquid in the numerical model was assumed to be incompressible, thus the pressure-based solver was selected for

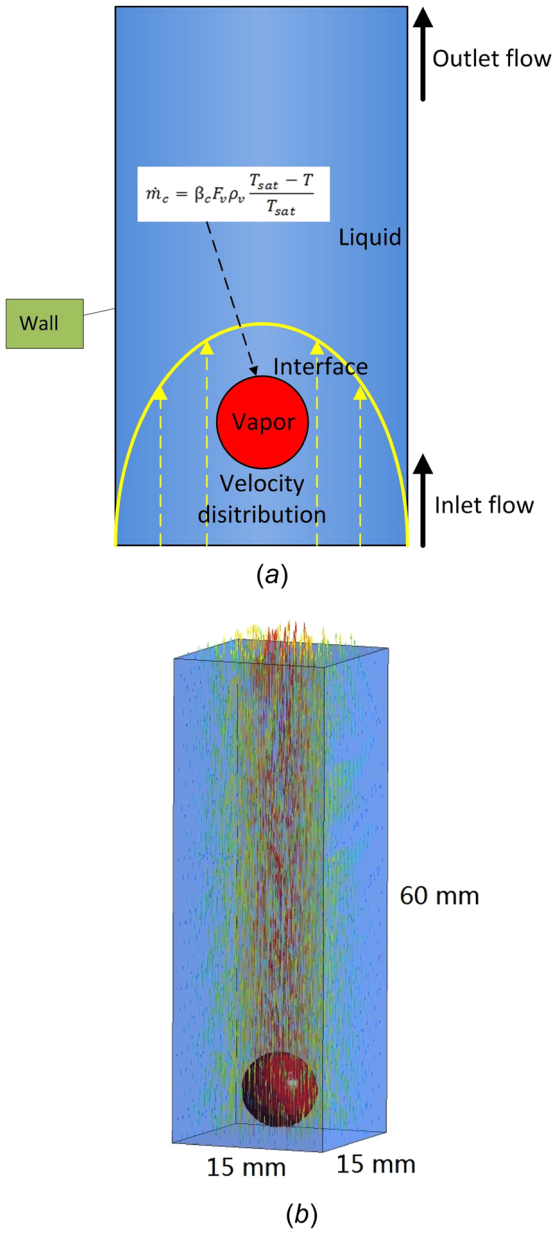

Fig. 1 CFD model; (*a*) boundary conditions and (*b*) 3D view (velocity vectors in the liquid)

the simulation. The PRESTO algorithm and upwind scheme of second order accuracy was adopted to discretize the pressure and the momentum and energy equations, respectively. Uniform grids were adopted to discretize the computational domain. The grid independency has been tested for various grid sizes to bubble diameter ratio in order to accurately predict the bubble surface deformations. With this treatment, the sensitivity analysis results show that numerical convergence can be achieved by setting the cell size to be about 1% of the initial bubble diameter. To keep the sharp interface, the PLIC was adopted in the model. The interface between two fluids was assumed to have a linear slope within each cell. The Geometric Reconstruction Scheme was used here. First, the calculation of position of the linear interface relative to the center was performed based on the newly predicted VOF. Next, the amount of fluid to be advected through each face was calculated using the computed interface representation. Normal and tangential velocity distributions on the faces were used as information in calculating the advection of fluid. Finally, the VOF in each cell was calculated through the balance of fluxes from the previous step.

The uniform meshes on the order of 10^{-4} m were generated in the three-dimensional Cartesian coordinate system, as shown in Fig. 2(*a*). The vapor–liquid interfacial region in condensation process is very complicated and its thickness is too small to be tracked. It is difficult to achieve both reasonable numerical efficiency and convergence at the same time. Especially as the bubble diameter decreases, the uniform mesh is not suitable for the bubble condensation simulation. In this study, the phase interface was assumed to be a saturated and movable boundary. A mesh adaption approach was applied to the liquid–vapor interface in the numerical model to obtain a better resolution of the interface change with a higher numerical efficiency, as shown in Fig. 2(*b*). The interface-cell is split into smaller ones and the accuracy can be improved obviously. The interfacial mesh size should be less than 1/16 of the bubble diameter, which can obtain the details of bubble condensation behavior [7]. In this study, interfacial mesh size was maintained 1/100 of the condensing bubble diameter. The condensing bubble was simulated using the VOF model coupled with the UDF of bubble condensation in ANSYS-FLUENT. The time steps used in the simulations were 10^{-5} s. And for each time step, the interfacial heat transfer was determined by the source terms described above.

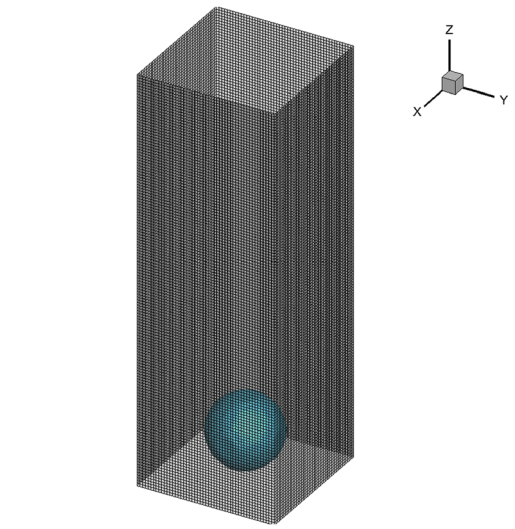

(*a*)

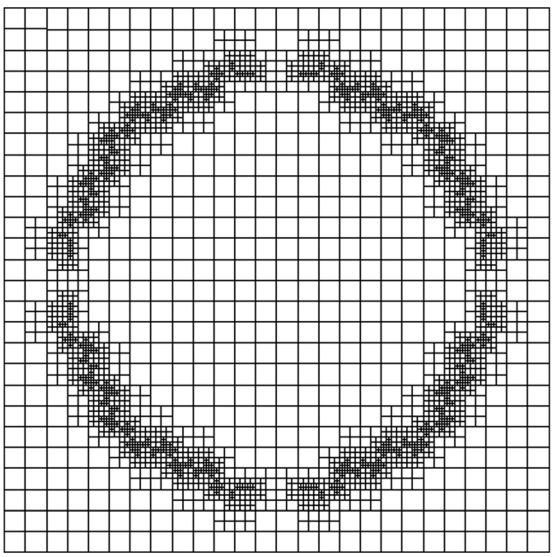

(*b*)

Fig. 2 The mesh in the computational domain; (*a*) uniform mesh and (*b*) the mesh in the computational domain

ANSYS-FLUENT was employed in this work to set up the numerical model, and the UDF was used extensively to solve the condensation heat and mass transfer. The simulation of the transient condensation process was performed using a personal computer with 3.0 GHz quad-core processor, 8 GB RAM. A calculation time of 100 hr was necessary to obtain the presented results.

Results and Discussion

In order to validate the numerical model, the results from open literature were used. The condensation behavior of a single bubble in subcooled boiling flow was numerically and experimentally studied in Ref. [7]. Figure 3 shows the bubble volume variations with time, which decreases due to the condensation. The numerical results for the condensation rate show good agreement with experimental data in Ref. [7]. It is ensured that the mass and energy source terms work well in the present VOF model.

The condensation heat transfer varies at every time step and mass transfer rate is different over each interface computational cell. In order to confirm the applicability of the developed CFD modeling with the VOF method, the sensitivity tests for the different bulk liquid temperatures and liquid velocities were performed, as shown in Table 1.

Figure 4 shows the visual results for the behavior of the condensing vapor bubble. When the condensation modeling is not applied, just the shape of bubble is deformed as time goes by without the change of bubble size. However, when condensation modeling is applied, the bubble condenses as the bubble rises up. It can be found that the bubble condenses more rapidly as the bulk liquid temperature decreases. It is obvious that the condensation heat can be transferred easily in the low temperature liquid flow.

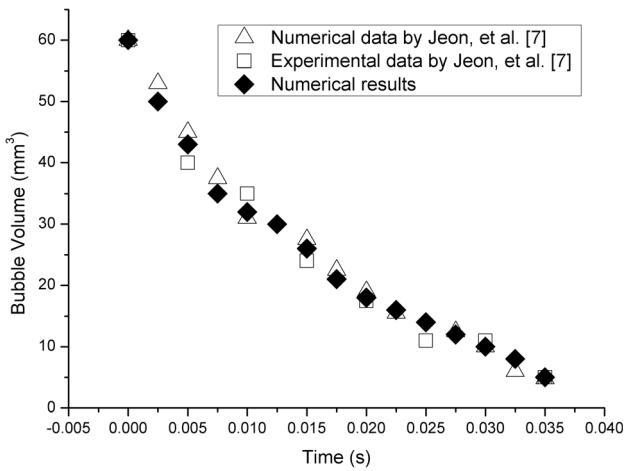

Fig. 3 Comparison of bubble volume with results in Ref. [7]

Table 1 Test conditions for 3D simulation

Case	Condensation Modeling	Liquid Velocity	Liquid Temperature	Bubble Diameter:
1	Not applied	0 m/s	373K	5 mm
2	Applied	0 m/s	358K	
3			363K	
4			368K	
5		0.1 m/s	363K	
6		0.2 m/s		
7		0.3 m/s		

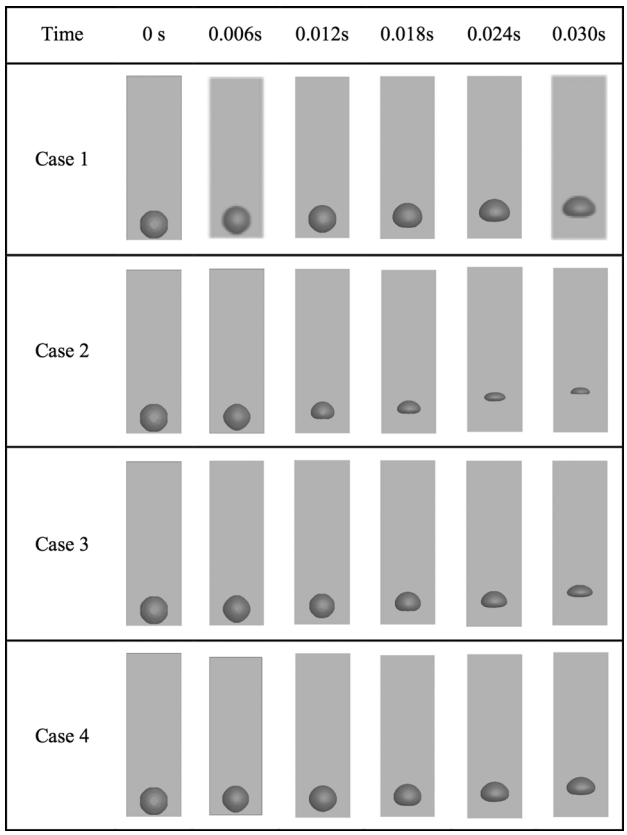

Fig. 4 Comparison of adiabatic and condensing bubble dynamics

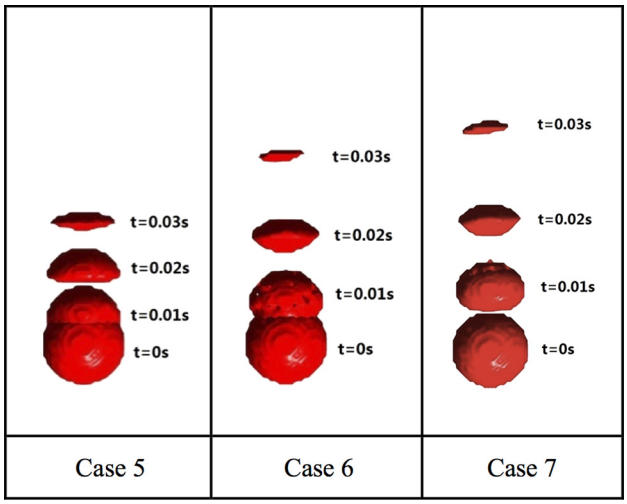

Fig. 5 Comparison of condensing bubble dynamics for different liquid water velocity

The temperature difference between the bubble and liquid is one influential factor needs to be considered in the subcooled flow boiling. Figure 5 represents the CFD simulation of the condensing bubble for different liquid velocities. The bubble rises up more rapidly in the channel and the moving distance increases during the bubble collapse as the liquid velocity increases. The changes of the bubble size increase as the liquid velocity increases. The liquid flow velocity is another influential factor needs to be considered in the subcooled flow boiling. As the liquid flow velocity near the vapor bubble increases, the condensation heat in the interfacial region is transferred faster by the convective way, which can enhance the bubble condensation process. Therefore, it can be concluded that the CFD modeling for the bubble condensation works well in the VOF model for the 3D simulations.

Figure 6(*a*) shows the cross section of the condensing vapor bubble in the subcooled boiling flow. Three regions exist in the cross section, which include the subcooled water, bubble interface and vapor bubble region. It should be noted that there is a high temperature region at the bottom of the bubble. This region implies that the condensation heat emitted from the interface warms up the subcooled water near the bubble as it condenses in the subcooled boiling flow, which proves that the energy source term works well in the VOF model. The temperature rise of the surrounding water by the condensation heat is remarkable at the bottom of the bubble although the condensation heat is given off from all around the bubble interface. As the bubble rises up in the subcooled water, the bubble pushes the water out so that the liquid circulation occurs, as shown in Fig. 6(*b*). Due to the liquid circulation, the heated water at the top of the bubble flows down along the bubble surface, then it is accumulated at the bottom of the bubble. As the condensation heat is transferred to the heated water in the bottom of the bubble continuously, the temperature of the water in this region gets higher than that of the water in the top or side region of the bubble. Finally, high temperature water is left in the bottom of the bubble as the thermal evidence of the rising bubble because the velocity of the heated water at the bottom of the bubble is lower than the bubble rising velocity.

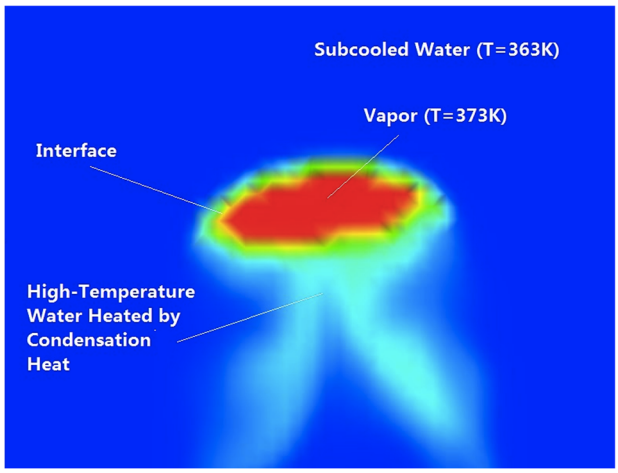

(*a*)

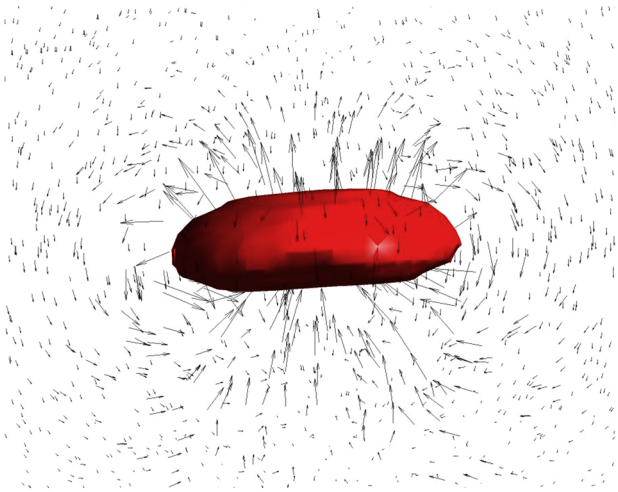

(*b*)

Fig. 6 Cross section of the condensing bubble; (*a*) temperature and (*b*) velocity vector in the subcooled boiling flow

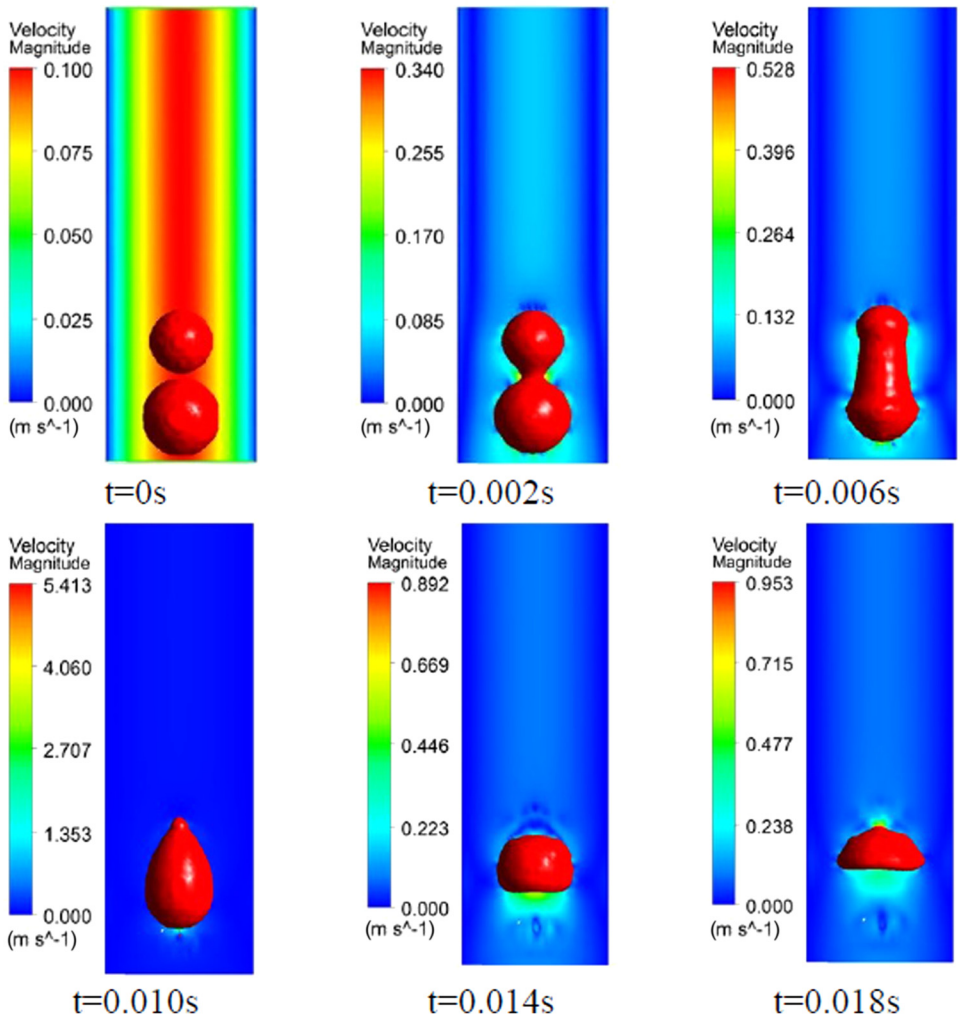

Fig. 7 Velocity distribution for merging process of two bubbles

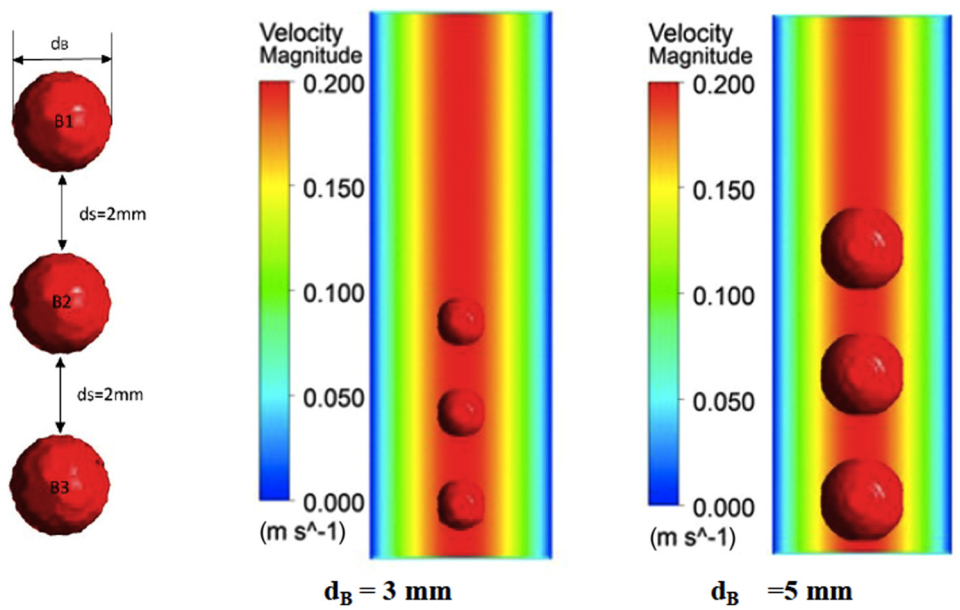

Fig. 8 Initial configurations (d_B = 3 mm and 5 mm)

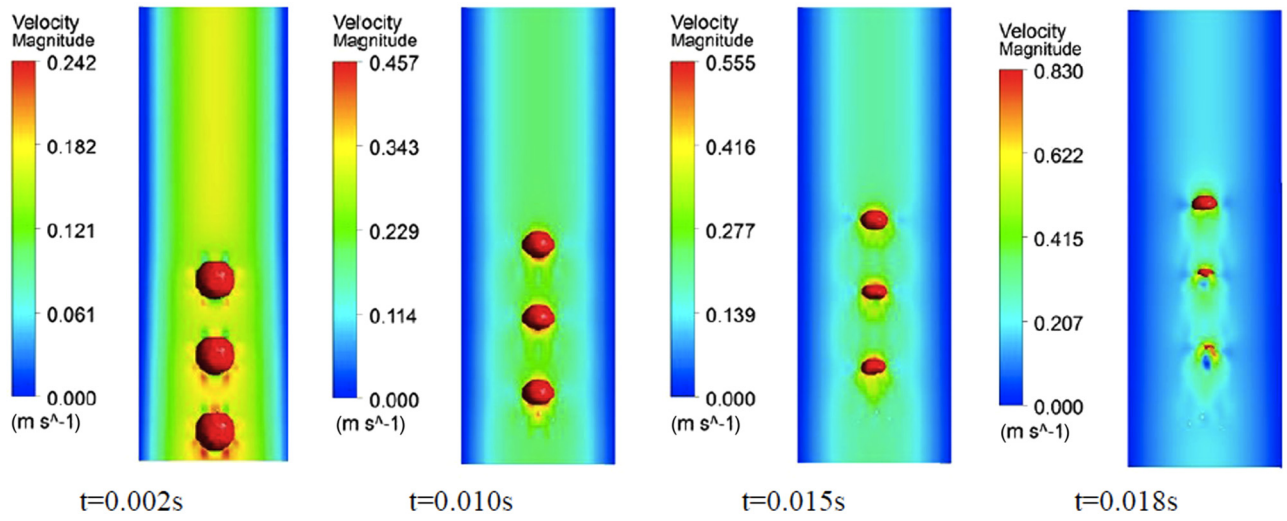

(*a*)

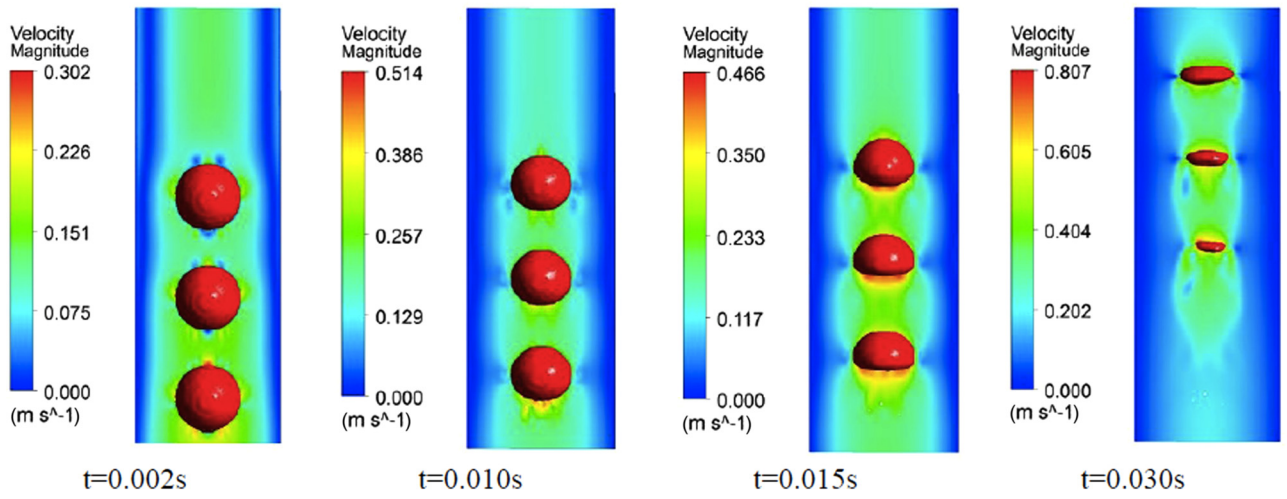

(*b*)

Fig. 9 Multiple bubbles condensation process for (*a*) $d_B = 3$ mm and (*b*) $d_B = 5$ mm at $V_{in} = 0.2$ m/s

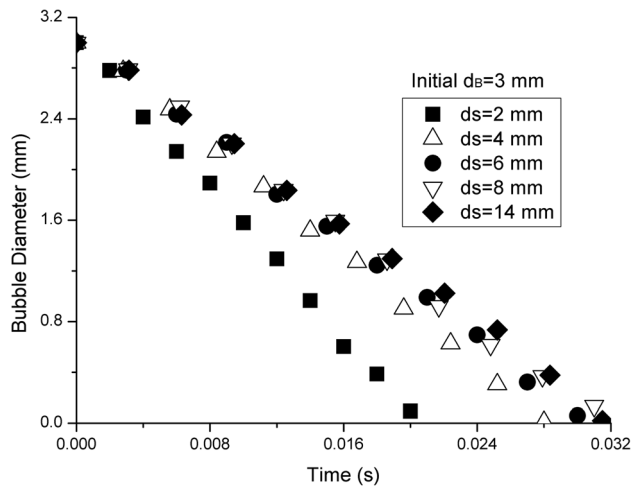

Fig. 10 Comparison of bubble diameters for different bubble distances

When the distance between two bubbles is very small, the two bubbles will merge to one big bubble first and the condensation process proceeds at the same time. The merging process is induced by the surface tension effect and different rising speeds, and the bubble shape deforms quickly. The liquid velocity near the bubbles increases as merging happens, as shown in Fig. 7, which enhances the condensation heat transfer.

The effect of neighboring bubbles on the condensation process was investigated by simulating three monodispersed bubbles condensing in liquid placed in a line ($d_B = 3$ mm and 5 mm), as shown in Fig. 8. The instantaneous bubble shapes and velocity distributions for different time intervals are shown in Fig. 9. During the condensation process, once the initial spherical shaped bubbles are deformed into the ellipsoidal bubbles, the influence of the neighboring bubbles is found to be obvious due to the random perturbation, which enhances the condensation heat transfer. A significant bubble deformation can be observed which leads to increased interactions between the bubbles. The ellipsoidal shape of the bubbles at the bottom is observed against the elongated shape of the bubbles in the middle and top. For the fixed bubble distance (2 mm) and different bubble diameters (3 mm and 5 mm), the same phenomena can be observed, i.e., for the lowest bubble

the rate of condensation heat transfer is higher than that for the other two. The water temperature and random perturbation are two main factors that have influences on the condensation rate of the lower bubble. The water temperature near the lower bubble increases due to the condensation heat emitted by the upper condensing bubble, which will decrease the condensation rate of the lower bubble. The random perturbation induced by the upper bubble can increase the condensation heat transfer of the lower bubble. It can be found that the effect of induced random perturbation is dominant in the condensation process when the lower bubble is influenced by the neighboring ones as evidenced by the quicker shrinkage of the lower bubbles in Fig. 9.

Numerical simulation was performed to determine the effect of bubble distance on the multiple bubbles condensation. The computational domain and initial condition were similar with that in Figs. 1 and 8, respectively, except that the height of the computational domain was extended to 200 mm to include all bubbles during the condensation process. Figure 10 shows the bubble diameter varies with time for different bubble distances, which are the bubble in the bottom (initial diameter is 3 mm) as shown in Fig. 8. It can be found that the bubble with smaller bubble distance condenses more quickly compared to that with a larger bubble distance. The influence of other bubbles on the condensation rate can be neglected if the distances between the bubbles are large enough. The local velocities of vapor and liquid are mainly influenced by the void fraction distribution in the flow domain, which directly determine the flow and heat transfer conditions. So the void fraction distribution can affect the pressure drop, flow stability and heat transfer rates in the heat transfer equipment. The knowledge of multiple bubbles condensation process is of importance in the prediction of void fraction distribution, which is fundamental in developing continuum models for the large-scale subcooled flow boiling.

Conclusions

Numerical simulations were performed to predict the behavior of the condensation of single and multiple bubbles. The condensation rate of a single bubble is influenced by the fluid velocity and the temperature difference between the bubble and fluid. For the multiple bubble case, the effect of interaction of the neighboring bubbles on the condensation process was analyzed based on the numerical predictions. The condensation rate of the lower bubbles increases due to the random perturbation induced by the upper bubbles. It can be concluded that the induced random perturbation dominates when the condensation rate of the lower bubble is influenced by the neighboring ones. The influence of neighboring bubbles on the condensation rate can be neglected if the distances between the bubbles are large enough.

Acknowledgment

This paper was supported by the National Natural Science Foundation of China through Grant Nos. 51306119 and 51376130 and the National Basic Research Program of China (973 Program) through Grant No. 2012CB720404. The Swedish Energy Agency also provided financial support.

Nomenclature

A = area, m^2
c_p = specific heat, J/(kg K)
d_B = diameter of bubble, mm
d_s = distance between bubbles, mm
D_s = Sauter diameter, m
D_{sm} = Sauter mean diameter, m
f = body force, N
F = volume fraction of fluid (VOF)
g = gravitational acceleration, m/s^2
h_i = interfacial heat transfer coefficient, $W/(m^2 K)$
Ja = Jacob number
k = thermal conductivity, W/(m K)
L = latent heat, J/kg
$\dot{m}_c$ = condensate mass flow rate per unit volume, $kg/(m^3 s)$
$\dot{M}_c$ = condensate mass flow rate, kg/s
Nu = Nusselt number
p = pressure, N/m^2
Pr = Prandtl number
q_T = energy source term, W/m^3
Q = energy, W
r = radius, m
R = universal gas constant, J/(mol K)
Re = Reynolds number
t = time, s
T = temperature, K
u = x-velocity, m/s
v = y-velocity, m/s
$\mathbf{V}$ = velocity vector, m/s
w = z-velocity, m/s
x, y, z = Cartesian coordinates

Greek Symbols

α_c = accommodation coefficient
α_i = volumetric interfacial surface area, 1/m
β_c = mass transfer time relaxation parameter, 1/s
κ = interface curvature, 1/m
μ = dynamic viscosity, kg/(m s)
ρ = density, kg/m^3
σ = surface tension, N/m

Subscripts

b = bubble
c = condensation
in = inlet
l = liquid
sat = saturated
v = vapor
vol = volumetric
x = x direction
y = y direction
z = z direction

References

[1] Revankar, S. T., 2013, "Heat Transfer Characteristics of Passive Condensers for Reactor Containment Cooling," ASME J. Therm. Sci. Eng. Appl., **5**(2), p. 021002.
[2] Kim, S. J., and Park, G. C., 2011, "Interfacial Heat Transfer of Condensing Bubble in Subcooled Boiling Flow at Low Pressure," Int. J. Heat Mass Transfer, **54**(13–14), pp. 2962–2974.
[3] Lucas, D., and Prasser, H. M., 2007, "Steam Bubble Condensation in Sub-Cooled Water in Case of Co-Current Vertical Pipe Flow," Nucl. Eng. Des., **237**(5), pp. 497–508.
[4] Lucas, D., Beyer, M., and Szalinski, L., 2010, "Experimental Investigations on the Condensation of Steam Bubbles Injected Into Subcooled Water at 1 MPA," Multiphase Sci. Technol., **22**(1), pp. 33–55.
[5] Inaba, N., Watanabe, N., and Aritomi, M., 2013, "Interfacial Heat Transfer of Condensation Bubble With Consideration of Bubble Number Distribution in Subcooled Flow Boiling," ASME J. Therm. Sci. Technol., **8**(1), pp. 74–90.
[6] Tian, W., Ishiwatari, Y., Ikejiri, S., Yamakawa, M., and Oka, Y., 2010, "Numerical Computation of Thermally Controlled Steam Bubble Condensation Using Moving Particle Semi-Implicit (MPS) Method," Ann. Nucl. Energy, **37**(1), pp. 5–15.
[7] Jeon, S. S., Kim, S. J., and Park, G. C., 2011, "Numerical Study of Condensing Bubble in Subcooled Boiling Flow Using Volume of Fluid Model," Chem. Eng. Sci., **66**(23), pp. 5899–5909.
[8] Eames, I., 2010, "Momentum Conservation and Condensing Vapor Bubbles," ASME J. Heat Transfer, **132**(9), p. 091501.
[9] Lucas, D., Frank, T., Lifante, C., Zwart, P., and Burns, A., 2011, "Extension of the Inhomogeneous MUSIG Model for Bubble Condensation," Nucl. Eng. Des., **241**(11), pp. 4359–4367.
[10] Ganguli, A. A., Pandit, A. B., and Joshi, J. B., 2012, "Bubble Dynamics of a Single Condensing Vapor Bubble From Vertically Heated Wall in Subcooled Pool Boiling System: Experimental Measurements and CFD Simulations," Int. J. Chem. Eng., **2012**, p. 712986.

[11] Jeon, S. S., Kim, S. J., and Park, G. C., 2009, "CFD Simulation of Condensing Vapo Bubble Using VOF Model," World Acad. Sci., Eng. Technol., **36**, pp. 209–215.
[12] Pan, L. M., Tan, Z. W., Chen, D. Q., and Xue, L. C., 2012, "Numerical Investigation of Vapor Bubble Condensation Characteristics of Subcooled Flow Boiling in Vertical Rectangular Channel," Nucl. Eng. Des., **248**, pp. 126–136.
[13] Pu, L., Li, H., Zhao, J., and Chen, T., 2009, "Numerical Simulation of Condensation of Bubbles Under Microgravity Conditions by Moving Mesh Method in the Double-Staggered Grid," Microgravity Sci. Technol., **21**, pp. S15–S22.
[14] Gopala, V. R., and van Wachem, B. G. M., 2008, "Volume of Fluid Methods for Immiscible-Fluid and Free-Surface Flows," Chem. Eng. J., **141**(1–3), pp. 204–221.
[15] Rabha, S. S., and Buwa, V. V., 2010, "Volume-Of-Fluid (VOF) Simulations of Rise of Single/Multiple Bubbles in Sheared Liquids," Chem. Eng. Sci., **65**(1), pp. 527–537.
[16] Warrier, G. R., Basu, N., and Dhir, V. K., 2002, "Interfacial Heat Transfer During Subcooled Flow Boiling," Int. J. Heat Mass Transfer, **45**(19), pp. 3947–3959.
[17] Liu, Z., Sunden, B., and Yuan, J., 2012, "VOF Modeling and Analysis of Filmwise Condensation Between Vertical Parallel Plates," Heat Transfer Res., **43**(1), pp. 47–68.
[18] Shi, D., Bi, Q., and Zhou, R., 2014, "Numerical Simulation of a Falling Ferrofluid Droplet in a Uniform Magnetic Field by the VOSET Method," Numer. Heat Transfer, Part A, **66**(2), pp.144–164.